Manuscript for submission to: *Mol Imaging Biol*

Evaluation of a flexible NOTA-RGD kit solution using Gallium-68 from different $^{68}Ge/^{68}Ga$-generators: pharmacokinetics and biodistribution in nonhuman primates and demonstration of solitary pulmonary nodule imaging in humans

Thomas Ebenhan[1]*, Isabel Schoeman[2]*, Daniel D. Rossouw[3]*, Anne Grobler[2], Biljana Marjanovic-Painter[4], Judith Wagener[4], Hendrik G. Kruger[5], Mike M. Sathekge[1] and Jan Rijn Zeevaart[2,4]

1 Nuclear Medicine, University of Pretoria and Steve Biko Academic Hospital, Pretoria, South Africa

2 Departments of Science and Technology, Preclinical Drug Development Platform, North West University, Potchefstroom, South Africa

3 Radionuclide Production Department, iThemba LABS, Somerset West, South Africa

4 Radiochemistry, The South African Nuclear Energy Corporation SOC Ltd (Necsa), Pelindaba, Pretoria, South Africa

5 Catalysis and Peptide Research Unit, University of KwaZulu Natal, Durban, South Africa

**Authors contributed equally to this manuscript*

Running title:

Flexible NOTA-RGD kit labeling procedure: biodistribution and clinical translation

For correspondence:

Jan Rijn Zeevaart, PhD
Scientific Head: Radiochemistry
Tel: +27 12 305 5786
Fax: +27 12 305 5944
Cell:+27-84-754-7834
Email: janrijn.zeevaart@necsa.co.za

Abstract

Purpose: Radiopharmaceuticals containing the motive tripeptide arginyl-glycyl-asparatic acid (RGD) are known to target αvβ3 integrins during tumor angiogenesis. A more generic kit radiolabeling procedure accommodating ^{68}Ga from different generators was developed for NOTA-RGD and evaluated for its versatile use and safety in subsequent *in vivo* applications. The [^{68}Ga]NOTA-RGD kit was further verified for its expected biodistribution and pharmacokinetics in nonhuman primates and its clinical sensitivity to detect solitary pulmonary nodules (SPN) in cancer patients.

Procedures: Single vial kits containing 28-56 nmol of NOTA-cyclo-Arg-Gly-Asp-d-Tyr-Lys (NOTA-RGD) and sodium acetate trihydrate buffer were formulated. Versatility of the NOTA-RGD radiolabeling performance and adaption to a TiO_2- and a SnO_2-based generator type, characterization and long-term storage stability of the kits were carried out. The blood clearance and urine recovery kinetics as well as the image-guided biodistribution of [^{68}Ga]NOTA-RGD was studied in a vervet monkey model. [^{68}Ga]NOTA-RGD kits were further tested clinically to target solitary pulmonary nodules.

Results: The kits could be successfully formulated warranting integrity over 3-4 months with a good [^{68}Ga]NOTA-RGD radiolabeling performance (radiochemical purity >95%, decay corrected yield 76-94%, specific activity of 8.8-37.9 GBq/μmol) The kits met all quality requirements to be further tested *in vivo*. [^{68}Ga]NOTA-RGD cleared rapidly from blood and was majorly excreted via the renal route. The liver, spleen, heart and intestines showed initial uptake with steadily declining tissue activity concentration over time. In addition, the [^{68}Ga]NOTA-RGD kit allowed for delineation of SPN from non-malignant lung tissue in humans.

Conclusions: A more versatile radiolabeling procedure using kit-formulated NOTA-RGD and different generator types was achieved. The uncompromised *in vivo* behaviour and efficient targeting of SPN warrants further investigations on the clinical relevance of [^{68}Ga]NOTA-RGD derivatives to implement initial guidelines and management of patients, with regard to integrin targeted imaging.

Key words:

Gallium-68, [^{68}Ga], RGD, $\alpha_v\beta_3$-integrin, NOTA-RGD, angiogenesis, PET/CT-imaging, peptide radiolabeling, lung cancer

Introduction

Lung cancer is still the leading cause of death amongst the different type of cancers worldwide [1-2]; it was newly diagnosed in about 1.61 million people and caused 1.38 million deaths [3]. The current epidemiologic pattern in Africa is making it more problematic: South Africa, for example has one of the highest rates of Human Immunodeficiency Virus (HIV) infection and the Acquired Immune Deficiency Syndrome (AIDS) [4] with HIV/AIDS related malignancies avidly increasing. In comparison to the general population, the incidence of lung cancer is two to four times higher in HIV patients [5]. It has been shown that lung cancer is one of the main risks that is diagnosed 4 to 27 months after the onset of AIDS [6]. In addition, advanced lung cancer, in stages III/IV, are currently diagnosed in ever-younger HIV-compromised patients [5]. Molecular imaging techniques such as combined positron emission tomography and computed tomography (PET/CT) can play a significant role in the management of those cancer patients. However, more clinical studies are needed to allow the manifestation of PET/CT imaging in radiotherapy planning as well as research and development of various radiopharmaceuticals including those tracers imaging the $\alpha_v\beta_3$ integrin expression during angiogenesis. Since 2012, the National Comprehensive Cancer Network (NCCN) proposed PET/CT scans for patient management instead of their previous approach of bone scintigraphy [7]. [^{18}F]FDG-PET is the gold standard for oncology imaging worldwide and the most frequently used radiotracer for imaging in cancer, RGD peptide based radiotracer provide the advantage of stratifying patients in need of targeted molecular therapies with antiangiogenic or $\alpha_v\beta_3$-targeted drugs as $\alpha_v\beta_3$ is a marker of activated, but not resting,[8-9] vessels and also available in most developing countries. Although there is continuous development of PET radiopharmaceuticals, very few are developed globally, they are not available in developing countries or they are not yet qualified for human administration [10]. The majority of the integrin targeting imaging tracers incorporate the tripeptide arginyl-glycyl-asparatic acid (RGD) which was identified as a cell-cell mediating motif used by extracellular matrix proteins [11]. The integrin $\alpha_v\beta_3$ is thereby considered a key feature of invasive tumor growth which makes it a potential biomarker of molecular imaging approaches to target tumor angiogenesis with non-invasive strategies. Multiple radiolabeled ligands have been introduced for imaging using PET, single photon emission tomography (SPECT), magnetic resonance imaging (MRI) or optical and sonographic techniques to visualize tumor angiogenesis or neo-vasculature [12-18].

PET, using RGD bioconjugates in particular, allows for a sensitive and specific visualization of *in vivo* biological processes of angiogenesis and integrin expression as RGD binds with high affinity to $\alpha_v\beta_3$ integrin [19]. Therefore several modifications of RGD were exploited to improve the pharmacological behaviour and the tumor accumulation *in vivo*, such as the synthesis of a cyclic monomer RGD [20] and for example, glycosylated for subsequent labeling with fluorine-18 [21]. Further, radiolabeled dimeric RGD was conjugated to macromolecules by using polyethyleneglycol (PEG_4) or tri-glycin (Gly_3) [22]. To introduce PET radiometal-based isotopes like ^{68}Ga, ^{89}Zr, ^{86}Y, ^{44}Sc or ^{64}Cu, a variety of RGD molecules were conjugated with a range of acidic bi-functional chelators such as 1,1,4,7,7-diethylene-triamine-pentaacetic acid (DTPA) [23], 1,4,7,10-tetraaza-cyclododecane-tetraacetic acid (DOTA) [24], 1,4,7-triaza-cyclononane-1,4-7-triacetic acid (NOTA) [25], 1,4,7-triaza-cyclononane,1-glutaric acid-4,7-acetic acid (NODAGA) [26] or 1,4,7-triazacyclononane phosphinic acid (TRAP) [27] without compromising the binding affinity of RGD.

In a recent summary the clinical applications of radiolabeled RGD peptides for PET imaging of integrin expression was reported [28] as follows: besides several technetium-99m and indium-111 labeled RGD derivatives, five radiofluorinated RGD-based radiodiagnostic agents, [^{18}F]Galacto-RGD, [^{18}F]Fluciclatide, [^{18}F]Alfatide, [^{18}F]RGD-K5, and [^{18}F]FPPRGD2, are currently under early clinical investigations for PET imaging. In addition, [^{68}Ga]NOTA-NCS-RGD and [^{68}Ga]NOTA-PRGD2 have also advanced clinically. There is a rapidly growing interest in the radiochemical community for the development of especially ^{68}Ga radiolabeled pharmaceuticals, as this is a generator-produced PET isotope, making radiopharmaceutical production relatively simple and very cost-effective. The [^{68}Ga]$Ga(Cl_4)^-$ intermediate, for example, forms an exceedingly stable complex with the NOTA chelator [29]. This demonstrates great clinical relevance when NOTA is used in labeling requiring a key-lock principle for the best diagnostic and therapeutic effect [30]. Geographically, countries with a smaller distribution of PET cameras can be challenged by very limited supplies of cyclotron produced isotopes. This makes research on generator-based radiopharmaceuticals a favourable alternative as it may be implemented in a hospital radiopharmacy setup. Different types of [^{68}Ge]/[^{68}Ga] generators are currently commercially available with column matrices including TiO_2, SnO_2 or organic ^{68}Ge-chelated coated silica, providing [^{68}Ga]Ga^{3+} for radiolabeling procedures. To date, these generator types are handled with different elution protocols and provide ^{68}Ga in various formulations [31].

Gallium-68-labeled RGD candidates need more in-depth investigations to determine their pharmacokinetics and clinical efficiency. Clinical studies on the differentiation of benign from malignant solitary pulmonary nodules (SPN) to determine if [^{18}F]FDG-PET can distinguish between the two types of lung nodules and tuberculosis were inconclusive [32]. Therefore, kit formulated NOTA-isothio-cyanatobenzyl-cyclo-Arg-Gly-Asp-d-Tyr-Lys (further denoted as NOTA-NCS-RGD), was kindly entrusted as a gift by Seoul National University for subsequent validation on the SnO_2-based [^{68}Ge]/[^{68}Ga]-generator used in South Africa. However, the provided radiolabeling procedure [25] was not applicable and was provided with limited information about the kit integrity, the thermodynamic compound stability and its compatibility towards other generator types. At this early stage of the introduction of kit formulated radiolabeling techniques for ^{68}Ga, these procedures are following very rigid protocols and may be challenged by ^{68}Ga eluted from the different generator types. Therefore we set out to evaluate a more accommodating kit procedure for NOTA-cyclo-Arg-Gly-Asp-d-Tyr-Lys (further denoted as NOTA-RGD). We herein report the preparation of NOTA-RGD kits to demonstrate the suitability for subsequent labeling with ^{68}Ga eluted from SnO_2- and TiO_2-matrix based generator types. Following the radioanalytical approval, the kit performance was verified for its expected biodistribution and pharmacokinetics in non-human primates (closing a crucial gap for the clinical translation of [^{68}Ga]NOTA-RGD) and its clinical sensitivity to detect solitary pulmonary nodules in cancer patients.

Material and Methods

Animals, Chemicals and Material

Vervet monkeys were obtained from a colony at the Onderstepoort Veterinarian Institute, Pretoria and inspected for general health to avoid occult infection. Kit formulated NOTA-NCS-RGD was provided by Seoul National University College of Medicine. A 5.2 mg batch of NOTA-RGD was purchased from FutureChem Co. Ltd (Seoul, Korea). Ultrapure grade hydrochloric acid (30-32 % HCl), trifluoroacetic acid (TFA) and methanol (MeOH) were purchased from Fluka Analytical (Steinheim, Germany). High-performance liquid chromatography (HPLC) grade water (resistivity = 18.2 MΩ cm) was produced in-house by a Simplicity 185 Millipore system (Cambridge, MA, USA). All other solvents were purchased, in at least HPLC grade, from Sigma Aldrich (Steinheim, Germany). Certified sterile pyrogen-free sealed borosilicate glass vials (5-30 mL) were provided by NTP Radioisotopes SOC Ltd.

(Pelindaba, South Africa) and were utilized for kit production, generator elution, and sterile saline dispension. Cartridges for solid-phase extraction (SPE) were obtained from Waters Corporation (Eschborn, Germany). Silica gel ITLC paper was purchased from Agilent Technologies (Forest Lakes, CA, USA). Sterile filters were obtained from Millipore (New York, NY, USA).

[^{68}Ge]/[^{68}Ga]-Generator Elution and Purification

^{68}Ga (i.e. gallium-68 or [^{68}Ga]$GaCl_3$), was routinely eluted from a SnO_2-based [^{68}Ge]/[^{68}Ga]-generator (1.85 GBq, IDB Holland, The Netherlands) by eluate fractionation with moderate acidic condition (0.6 N HCl) assembling the [^{68}Ga]-activity in 2 mL eluate (reference method). For inter-comparison, radiolabeling (N = 4) was carried out with ^{68}Ga eluted from a TiO_2-based [^{68}Ge]/[^{68}Ga]-generator (1.1 GBq, Eckert & Ziegler, Germany) using lower acidic conditions (0.1 N HCl). A 7.5 mL eluate was subsequently mixed with 30% HCl to yield a molarity > 5.5 M. A strong anionic DOWEX resin (50WX8; 100-200 mesh, Fluka Analytics, Steinheim, Germany) was used to purify the activity solution from potentially co-eluted metals and germanium-68. The resin-bound [^{68}Ga]-activity was desorbed with ultrapure water and assembled in 0.85 mL acidic solution (+SAX method). Alternatively, a fractionated elution similar to the reference method was performed on the TiO_2-based [^{68}Ge]/[^{68}Ga]-generator (-SAX method). Elutes form both generators used were within the first 6 months of the generator's lifespan.

Gallium-68 Radiolabeling of NOTA-RGD

NOTA-RGD was labeled directly for optimization using a radiolabeling procedure, which amended a previously described method by Rossouw et al. [33]. Briefly, 2.5 M sodium acetate buffer (or equivalent milligram of sodium acetate salt) was added to the [^{68}Ga]-eluate to obtain a pH of 4-4.5 and 0.25-1.5 mL of this buffered [^{68}Ga]-eluate was used for labeling. After adding 5.6 - 56 nmol NOTA-RGD, the mixture was stirred for 20-30 s. The reaction vial was allowed to incubate at ambient temperatures and subsequently at 90 ºC for 5-10 min, to address the benefit of a heating step on the radiochemical yield of [^{68}Ga]NOTA-RGD. Small aliquots were continually removed for quality control purposes.

In-house Kit Vial Manufacture of NOTA-RGD

Sterile cGMP kit vials were manufactured at Radiochemistry (Necsa, Pelindaba) using a 5 mL certified vials (NTP Radioisotopes SOC). A peptide stock solution of 1 mg/mL NOTA-

RGD in Millipore water was prepared. Aliquots of 60 µL were transferred into the glass vials (K60 kits 56 nmol; final peptide concentration 34 µM). Alternatively, kits with reduced NOTA-RGD content were produced (K30 28 nmol; final peptide concentration 17 µM). All kits were supplemented with 400 µL of a 2.5 M sodium acetate trihydrate buffered solution followed by ad-hoc freezing (Bio-Freezer, Thermo Fisher Scientific, Waltham, MA, USA) and the subsequent transfer to an Alpha 1–5 laboratory freeze dryer (Christ, Osterode am Harz, Germany) where lyophilisation was carried out overnight under an argon atmosphere at 0.05 mbar. The vials were sealed and routinely stored either at room temperature, 2–8 °C, -15 °C or -50 °C to assess kit shelf integrity and thermodynamic stability (based on radiolabeling performance).

Kit Vial-based Gallium-68 Radiolabeling

The NOTA-NCS-RGD kit was labeled as described elsewhere [25]; 15 kits from three batch productions, each comprising of 10.7 µg (10 nmol) NOTA-NCS-RGD and 15.4 mg (108 µmol) Na_2HPO_4 buffer, were studied. In contrast, an "in-house"-developed method (see aforementioned sections) facilitated the NOTA-RGD kit labelling. Briefly, the kit vial was punctured by a Jelco 22G x 1'' polymer catheter (Smiths Medical, Croydon, South Africa) to allow non-metallic transfer of the [^{68}Ge]/[^{68}Ga]-generator eluate into the reaction vial. The kits were than stirred for 20 s and incubated for 10-15 min at 90 °C. Small aliquots were continually removed for quality control purposes.

Purification of [^{68}Ga]NOTA-RGD

Disposable solid-phase extraction (SPE) units (C18 500 mg 3 cc vac and C18 light 100 mg, Waters, Eschborn, Germany) were employed; preconditioning with absolute ethanol was followed by deionized water treatment. SPE C18 light units were utilized for purification of small sample volumes (for subsequent preclinical tracer administration), whereas SPE C18 500 mg units were used for purification of upscaled tracer production. All crude peptide samples were loaded with a flow rate of 2 mL/min followed by 0.5-1 mL saline solution which was used to rinse the reaction vial to harvest residual gallium-68 labeled peptide. SPE units were subsequently washed with saline solution. To recover any product related activity, the SPE units were treated with 1-3 mL of a saline/ethanol mixture (90:10 v/v) and additionally with a saline/ethanol mixture (80:20 v/v) before draining with ≤ 1 mL saline solution from residual liquid and measured for retained radioactivity. If required, the

[^{68}Ga]NOTA-RGD solutions were sterile-filtered through a 0.22 µm membrane using a low protein-binding filter.

The radiochemical performance assessment on the quality of the of the cold and radiolabeled kits included tests and calculation on the following parameters: sterility, pH value of the reaction mixture and product solutions, radiochemical purity (%RCP), percentage radiolabeling efficiency (%LE), decay corrected activity yield (%RCY), radiochemical integrity, thermodynamic stability and labeling reproducibility.

Chromatographic Analysis [^{68}Ga]NOTA-RGD

Instant Thin Layer Chromatography (ITLC) was conducted to determine the %LE and %RCY as described elsewhere [25, 34]. Briefly, ITLC-SG paper (Agilent Technologies, Forest Lakes, CA, USA) was used as stationary phase and spotted with the [^{68}Ga]-peptide solution, followed by exposure either to the mobile phase (0.1 M citrate, pH 5) or to 1 M ammonium acetate/methanol (1:1 v/v) for determination of product yield, purity and [^{68}Ga]-colloid formation. The activity distribution was analyzed by a gamma detector equipped TLC scanner (Veenstra, the Netherlands); peak identification and quantification was possible by an "area under the curve" analysis.

High Performance Liquid Chromatography (HPLC) analysis was carried out to determine the labelled compound and %RCP using an Agilent 1200 series instrument (Agilent Technologies Inc., Wilmington DE, USA), diode array detector (DAD) and radioactive detector (Gina Star, Raytest, Straubenhardt, Germany). A Phenomenex Luna C18 column was used (250 x 4.6 mm, 5 µm). The mobile phase consists of (A) 0.1% TFA in water and (B) 0.1% TFA in acetonitrile; gradient elution of 0-2 min 5%B and 2-32 min 65%B was conducted. Column temperature and flow rate were set on 40 °C and 1.0 mL/min respectively. Unbound [^{68}Ga]Ga^{3+}, [^{68}Ga]$GaCl_4^-$ and [^{68}Ga]$Ga(H_2O)_6$ were eluted at 2.3-4 min, whereas [^{68}Ga]NOTA-RGD was eluted at 11.4-12.5 min. The retention times of the crude and SPE-purified compounds were compared to each other and to their respective UV signals. No reference standard was used as the RGD material was purchased as certified > 95.8 % purity and the certificate indicated a Mol.Wt= 1184.18 and ESI-mass 1069.47 as determined with HPLC-MS.

Image –guided Biodistribution of [^{68}Ga]NOTA-RGD in Non-human Primates

The imaging studies in primates were conducted according to the South African code of practice for the care and use of animals as ethically approved by the Animal Use and Care Committee of the University of Pretoria (Ref BRC-001-09). Three male vervet monkeys (Cercopethicus aethiops) were kept in separate cages and the University of Pretoria Biomedical Research Centre (UPBRC) provided husbandry and management practices with emphasis on environmental enrichment to optimize the health and mental status of the animals. The animals were fed a balanced diet, allowed access to water *ad libitum* and were fasted for 12 h prior to the study. Subcutaneous injections of 10 mg/kg of Ketamine Hydrochloride 100 mg/mL (The Premier Pharmaceutical Company, Bryanston, South Africa) and 0.5 mg/kg of Midazolam 5 mg/mL (Roche Products Pty Ltd., Isando, South Africa) was used for immobilisation. Induction of anaesthesia was achieved by a bolus injection of 6% sodium pentobarbitone solution until the surgical plane of anaesthesia was reached; maintenance was supported by an infusion pump running a pre-calculated flow rate of the anaesthetics. Monkeys were intubated to warrant controlled breathing and the heart rate was recorded using electrocardiographic monitoring. During PET/CT image acquisition the arterial blood pressure was monitored via a femoral artery port. Each of the three animals used was allowed three static whole body PET/CT scans starting at either 30 min, 60 min, 90 min or 120 min with the animal in supine position following intravenous administration of [^{68}Ga]NOTA-RGD. After imaging (no later than 150 min p.i.), the animals were allowed to recover from the anaesthesia and were kept in an isolation unit overnight to eliminate the radioactivity.

Image Acquisition, Reconstruction and Quantification

A clinical PET/CT camera (Siemens Biograph True Point, 40 slice CT) was used for image acquisition. Images were acquired in three-dimensional (3D) list mode and reconstructed with and without attenuation correction (CT-based) using ordered subset expectation maximization to yield axial, sagittal, and coronal slices (CT parameters: 80-120 kV, 100 mA, slice thickness 5 mm, 0.8 mm pitch, matrix size 512 x 512). All images were first evaluated qualitatively followed by semi-quantification analysis using Siemens ESoft software on MI Processing workstation (version 2.0.21; ABX GmbH, Dresden, Germany). 3D volume of interests (VOIs) were drawn manually surrounding all relevant organs or tissues and their activity concentrations were expressed as standardized uptake value (SUV = [activity per mL tissue] / [injected activity per body weight], g/mL). Additional images for illustration

purposes were processed with courtesy of Siemens International (Erlangen, Germany) on a Multimodality Work Place using Software version VE52A with Fused Vision 3D.

Blood Clearance and Urinary Recovery of [^{68}Ga]NOTA-RGD in Nonhuman Primates

Blood samples (0.5-1.5 mL) were collected from the cephalic vein in pre-weighed heparinised tubes following administration of the radioactive tracer at different time intervals up to 60 min. Urine (volume available at point in time ≤20 mL) was collected in pre-weighed screw cups from catheterized bladders at different time intervals up to 120 min. All samples were weighted; radioactivity was measured using a CRC 25 dose calibrator (Capintec Inc., USA) and decay corrected. The total urine recovery was calculated uniting all samples up to 120 min. Data points were used to draw time-activity curves to determine the circulation (pharmacological half-life) and excretion (urinary elimination rate) of the radiopharmaceutical.

Clinical [^{68}Ga]NOTA-RGD Kit Performance in Humans

Approval was granted by the University of Pretoria's Research Ethics committee and has been conducted in accordance with the ethical standards laid down in the 1964 Declaration of Helsinki and its later amendments. Written informed consent was obtained from the patients prior to tracer injection and imaging. The image acquisition protocol did not involve any special requirements or activities.

An intravenous bolus of [^{68}Ga]NOTA-RGD was administered followed by 200 mL 10% Gastrografin (Bayer, Austria), given oral 30 min ahead of imaging and 100 mL Iopamidol 370 (Bracco, Courcouronnes, France) given as intravenous contrast at a 2 mL/s flow rate, 1 min ahead of the CT scan. Three patients with confirmed malignant lung pathology underwent static [^{68}Ga]NOTA-RGD-PET/CT at 60 min after tracer injection. Image acquisition and reconstruction was carried out as described earlier. The normal tracer biodistribution was measured in arterial blood, thyroid, heart, lung, liver, spleen and bone marrow. Potential pulmonary lesions were represented as maximum standard uptake value (SUVmax) or averaged over all potential detected lesions.

Statistical Analysis

If systematic errors were non-existent, outliers were determined by the *Grubbs test*. If not stated otherwise, data was expressed as mean values ± standard deviation (SD) using Origin

Lab Pro 8.1 or Microsoft Office Excel software. Standard error of mean (sem) was occasionally utilized to express populations of datasets concerning radiolabeling and clinical data. The significance of two mean values was calculated by the *Student's-t-test* (paired and unpaired comparison). The level of significance was set at $P \leq 0.05$. Results concerning the kit integrity as well as the blood and urine concentration were analyzed using linear regression, and the agreement was verified through the correlation coefficient (R^2).

Results

Optimization of NOTA-RGD Molarity for Kit Formulation

HPLC and ITLC analysis of radiolabelling results achieved with the NOTA-NCS-RGD kits from Seoul National University (see supplementary information for details) indicated that kit optimisation was required. Prior to kit formulation, manual radiolabeling using 10 µg NOTA-RGD amounted to 31 ± 3 %LE (N =4). For improvement, kits containing 30 µg (K30) or 60 µg (K60) were compared with manual radiolabeling procedures adding 30 µg (NK30) or 60 µg (NK60) to the buffered generator eluate solution. Levels of ^{68}Ga colloid formation were reduced for both, K30 (P =0.073) and K60 (P =0.081) compared to manual [^{68}Ga]NOTA-RGD labeling (NK30 and NK60; **Fig. 1a**). Significant higher radiolabeling was achieved using K30 (P =0.01) or K60 (P =0.00017) kits over manual radiolabeling of NK30 and NK60 (**Fig. 1b**). Neither the amount of colloid formation (P = 0.225) nor %LE (P = 0.139) differed between K30 (N =4) and K60 (N =7) kit radiolabeling.

Generator Eluate Purification and NOTA-RGD Kit Radiolabeling

NOTA-RGD kits (K60) were successfully labeled with ^{68}Ga eluted from SnO_2- and TiO_2-based generators (**Tab. 1**). Both generators provided a similar yield of [^{68}Ga]$GaCl_3$ and the complete labeling procedure, including quality control, was achieved in 34 and 38 min (reference and –SAX, fractionated elution applied) or 43 min with implementing anion exchange pre-purification (+SAX) of the [^{68}Ga]-eluate solution. Results indicate both substantial reduction of colloid formation (P <0.05) and a slight increase in the %LE (P =0.098) for ^{68}Ga-NOTA-RGD utilizing a pre-purified generator eluate.

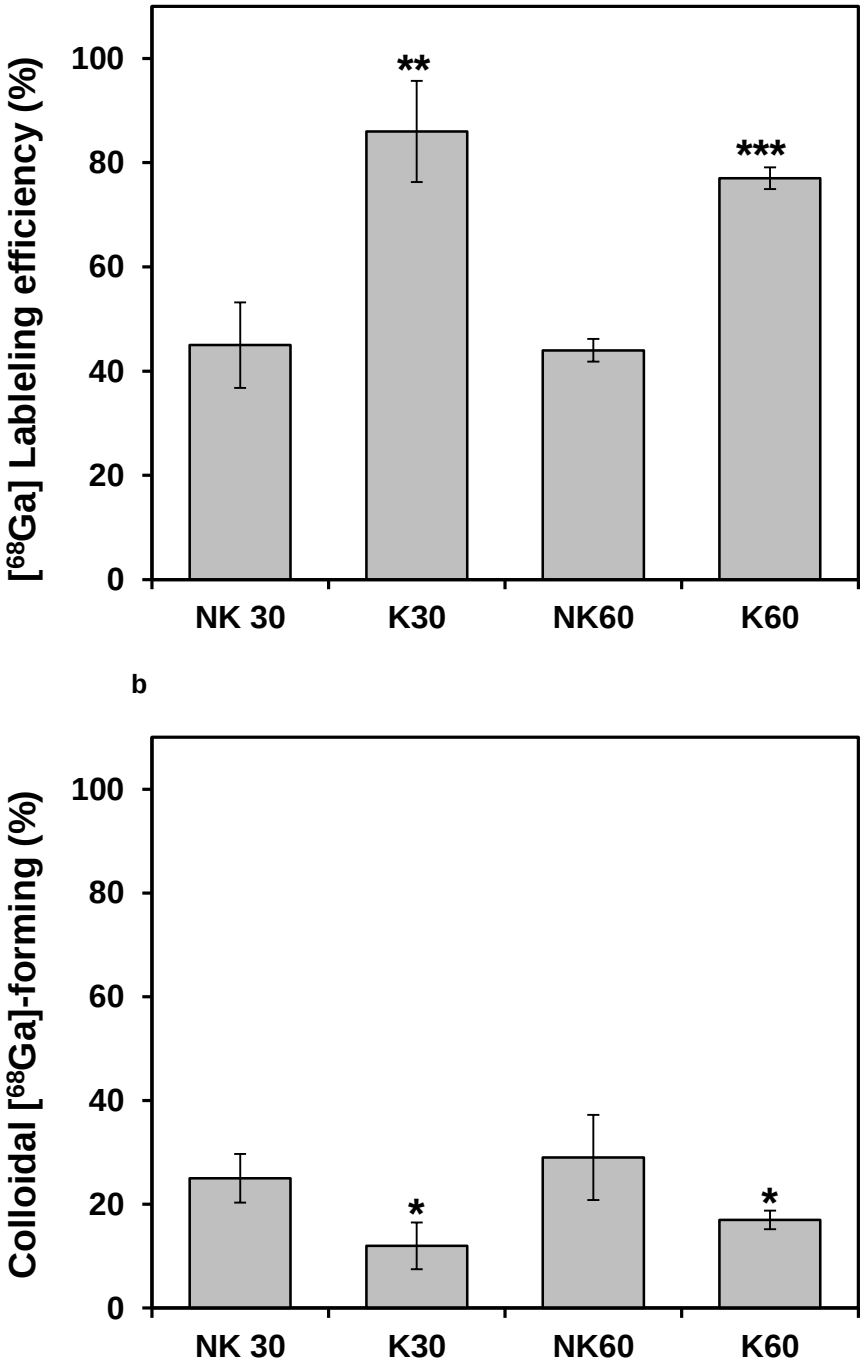

Fig.1 NOTA-RGD kit radiolabeling performance. Comparison of (**a**) labeling efficiency and (**b**) colloid formation of direct (manual) NOTA-RGD radiolabeling (NK30 and NK60) with freshly produced cGMP NOTA-RGD kits (K30 and K60). Results are expressed as mean ± sem of N ≥ 4 individual tests expressed as percentage of added [^{68}Ga]-activity; unpaired *Student's t-test* returned *P* values (*) ≤0.07, (**) <0.01 and (***)<0.001 comparing NK- with K-groups.

Table 1. Influence of generator eluate purification on [^{68}Ga]NOTA-RGD radiolabeling

		[^{68}Ga]NOTA-RGD radiolabeling		
Elution method[#]		**FE (Reference)**	**FE, + SAX**	**FE , - SAX**
Generator type		iThemba 50 mCi		Eckert & Ziegler 30 mCi
Solid matrix material		SnO_2		TiO_2
Mobile phase		0.6 N HCl		0.1 N HCl
Generator shelf life span (d)		96 - 140	124 - 134	101 - 108
Yield [^{68}Ga] (%)		94 ± 2 (n = 7)	81 ± 4 (n = 11)	90 ± 1 (n = 7)
[^{68}Ga]-elution discharge (%)	**bound**	-	8.6 ± 4.0	-
	liquid	5.9 ± 1.9*	8.5 ± 2.9	10.2 ± 1.3
ITLC	**Crude labeling (%LE)**	71 ± 6	81 ± 4	74 ± 5
	RCP (%)	99 ± 0.50	99 ± 0.33	99 ± 0.25
	Colloids (%) loss	8.0 ± 2.0	4.5 ± 2.2*	8.5 ± 3.8
Sep Pak (%) loss		13 ± 2	12 ± 2	13 ± 3
Duration (min)		38 ± 2	43 ± 2	34 ± 4

[#]) Elution method: fractionated elution (FE) combined with (+SAX) and without (-SAX) eluate purification followed by standard labeling procedure were applied (see more details in "Material and Methods Section"). Values are expressed as mean (± SD; N ≥ 3),
*) *Student's-t-test* returned a significant difference between generator types ($P \leq 0.05$).

Purification (Solid Phase Extraction)

After kit-based radiolabeling, SPE units were evaluated for optimal purification of [^{68}Ga]NOTA-RGD from free [^{68}Ga]$(Cl_4)^-$, [^{68}Ga]$(H_2O)_6$ and colloidal [^{68}Ga] (**Tab. 2**). Both SPE types showed high total desorption levels with alcoholic saline solutions, amounting to a total percentage of adsorbed activity of 89 ± 3% and 76 ± 5% for SPE C18 (500 mg 3 cc vac) and SPE C18 (light), respectively. Significant higher amounts of activity was desorbed with 10% alcoholic saline solution (P = 0.049), hence, significant lower SPE-bound activity (P =0.038) occurred for SPE C18 (500 mg 3 cc vac) over the C18 light cartridge. For preclinical application the SPE elution with the ethanol/saline (20:80 v/v) protocol was

voided to achieve the minimum solvent levels for ethanol in the final injection solution. The purified [^{68}Ga]NOTA-RGD solution showed a stable shelf-life over the 120 min tested. The product radioactivity achieved was 204 ± 44 MBq (N =10); the %RCP of [^{68}Ga]NOTA-RGD determined by HPLC was 99.2 ± 0.54% (N =11). Samples showed negligible traces of [^{68}Ge] (≤0.0004%), cationic metal impurities (0.05 – 9.1 ppm) and no turbidity. The calculated percentage of ethanol was 2.0-2.5% in the final radiopharmaceutical product solution. [^{68}Ga]NOTA-RGD K60 kits labeled at an average specific activity of 15.8 GBq/µmol (Range: 8.8-37.9 GBq/µmol) depending on the amounts of NOTA-RGD and ^{68}Ga added. The average full-scale specific activity based on the herein reported kit performance is calculated as 19.7 ± 5.5 GBq/µmol. During ITLC-SG analyses, the activity corresponding to the [^{68}Ga]NOTA-RGD complex remained at the point of spotting (R*f* = 0–0.1), while uncomplexed [^{68}Ga] moved toward the solvent front with an R*f* = 0.8–0.9 under identical conditions.

Table 2. Performance of SPE purification on K60 [^{68}Ga]NOTA-RGD kit vial radiolabeling

SPE Sep Pak Type		**C18 500 mg 3 cc vac column** [#]	**C18 light (100 mg) online cartridge** [#]
Adsorbed Activity (AA) (MBq)		250 ± 64	119 ± 10
Total SPE Elution (% AA)		89 ± 3	76 ± 5
Product Fraction % Ethanol / Saline (v/v)	10 / 90 (v/v)	77 ± 4*	63 ± 5
	20 / 80 (v/v)[$]	12 ± 1	13 ± 1
Retained Activity (% Range AA)		4-13*	15-37

Values are expressed as mean (± sem; N = 4).
[#]) Analysis of K60 kits with ≤ 90 days shelf lives were considered.
[$]) Measurements reflect activity percentage separate from the 10/90 (v/v) fraction.
*) *Student's t-test* returned a significant difference between cartridges (*P* ≤ 0.05).

Kit stability

A strong dependency was observed comparing gallium-68 labeling of NOTA-RGD kits (K60) that were stored at different temperatures (**Fig. 2**). Initial radiolabeling was sufficiently high for kit vials that were kept frozen in the first week after manufacturing (>89 %LE for -15 °C and >93 %LE for -50 °C). In contrast, kit vials that were kept at 2-8 °C performed significantly lower radiolabeling of NOTA-RGD (approx. 66 %LE) and kept decreasing to

<30 %LE within less than 200 d. HPLC/ITLC analysis, at that stage, detected >52% compound losses (SPE unit and colloid formation) and radiolabeled by-products presuming kit decomposition. Kit vials that were long-term stored at -50 °C performed significantly better than kit vials stored at fridge temperatures ($P < 0.001$), sustaining a >85 %LE and >70 %LE for a duration of 180 d and 400 d, respectively. In comparison, kit vials stored at -15 °C showed insignificant differences in radiolabeling ($P = 0.408$), warranting a >70 %LE and >50 %LE over a duration of 150 d and 300 d, respectively.

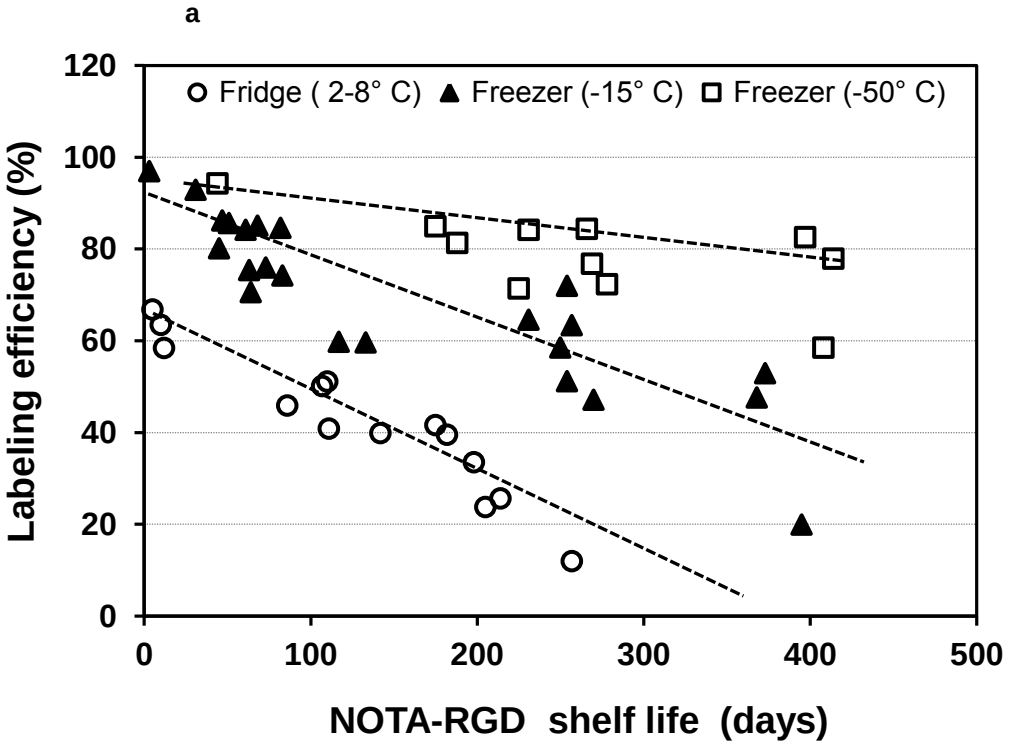

Fig. 2 Impact of storage temperature on the NOTA-RGD kit integrity. Results are presented as percentage labeling efficiency related to the added [^{68}Ga]-activity from individual radiosynthesis with NOTA-RGD kits of increasing shelf life. Samples stored at fridge temperatures (2-8 °C, open circles, R^2=0.91, N = 14) were compared with frozen kit vials kept at -15 °C (closed triangles, R^2=0.77, N = 23) and -50 °C (open squares, R^2=0.41, N = 11).

PET /CT Imaging-guided Tracer Distribution in Non-human Primates

Monkeys of 5.8-7.0 kg received a dose of 13.6 ± 3.3 MBq/kg [^{68}Ga]NOTA-RGD. Static PET/CT images were acquired at 30 min (N = 1), 60 min (N = 3), 90 min (N = 1) and 120 min (N = 2) after tracer injection and the activity concentration in target organs and tissues were quantified as SUV(mean) (Table 3). The 3D-rendered PET/CT images (**Fig. 3**), acquired 60 min post-injection of ^{68}Ga-NOTA-RGD, indicate the majority of activity was observed in the kidneys, urinary bladder and liver. The spleen, heart and bone marrow show moderate initial uptake with subsequent declining organ activity concentration. Minimal activity uptake was observed in the musculoskeletal tissue and brain; there was also no

significant difference between the SUV values of triceps and quadriceps muscles at 60 and 120 min. The tracer concentration in all other organs and tissues were significantly smaller ($P < 0.05$) than the muscle tissue (**Tab. 3**).

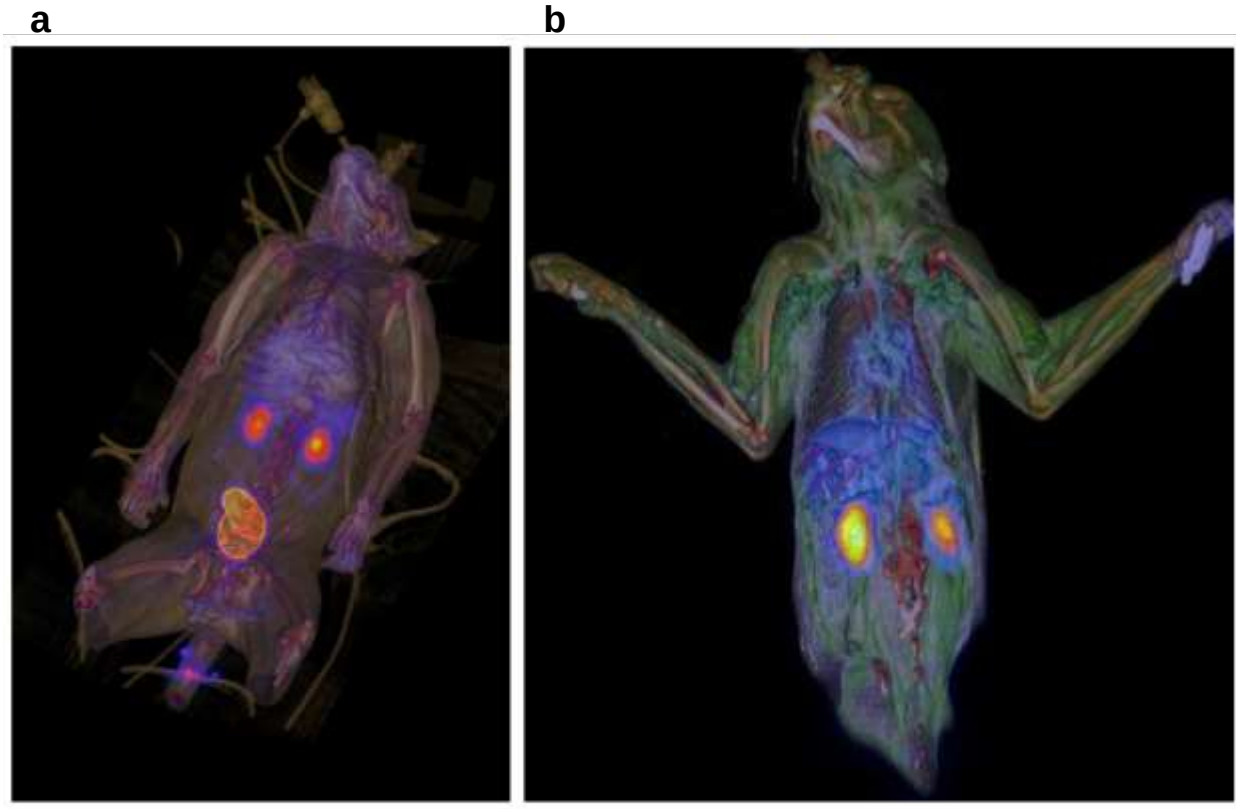

Fig. 3 PET/CT image-guided [^{68}Ga]NOTA-RGD biodistribution in non-human primates. Representative three-dimensional rendered PET/CT image projections: (**a**) whole body bone-weighted and (**b**) soft tissue-weighted (skull to abdomen), acquired 60 min post intravenous injection of 13.6 ± 5.8 MBq/kg [^{68}Ga]NOTA-RGD (N = 3). Images were processed using Multimodality work place software version VE52A with fused vision 3D (provided by Siemens International, Erlangen, Germany).

Table 3. Organ and tissue concentration of [^{68}Ga]NOTA-RGD in non-human primates; SUV quantification from PET/CT imaging

Organ/ Tissue	Standardized uptake value (SUV)			
	30 min p.i.$^{\#}$	60 min p.i.‡	90 min p.i.$^{\#}$	120 min p.i.$^{\$}$
Heart	1.01	0.89 ± 0.32	0.62	0.35 ± 0.12*
Liver	1.24	1.7 ± 0.70	1.91	0.49 ± 0.08*
Spleen	1.22	1.6 ± 0.49	1.39	1.1 ± 0.60
Intestines	1.03	0.86 ± 0.29	0.60	0.49 ± 0.13*
Bone (scapula)	0.36	0.43 ± 0.12	0.38	0.39 ± 0.09
Brain	0.04	0.04 ± 0.02	0.05	0.07 ± 0.01
Kidneys	3.53	3.2 ± 0.88	2.78	1.9 ± 0.60
Urinary bladder	25	31 ± 15	24	24 ± 3.4
Quadriceps muscle	0.19	0.24 ± 0.04	0.22	0.22 ± 0.04
Triceps muscle	0.18	0.23 ± 0.05	0.22	0.22 ± 0.03
Background	-	0.04 ± 0.005	-	0.03 ± 0.003

Values expressed as mean SUV (±sem) for ‡) N = 3; $^{\$}$) N = 2, $^{\#}$) N = single animal.
*) *Student's- t-test* returned a significant difference between SUV at 60 min and 120 min post injection ($P \leq 0.05$).

Blood Clearance Kinetics and Urinary Recovery of [^{68}Ga]NOTA-RGD

The time dependent concentration of [^{68}Ga]NOTA-RGD measured from individually taken blood samples (N = 10) was further optimized by applying a mathematical data smoothing algorithm (Savitzky-Golay, Origin Pro 8, OriginLab Corporation, Northampton). The results of the fluid analysis of [^{68}Ga]NOTA-RGD confirmed that the peak blood activity concentration was obtained 1 min after injection, amounting to 0.75 ± 0.07 %ID/g (**Fig. 4a**). Activity cleared quickly from the blood pool with a exponential decrease of the initial activity within the first 45 min ($R^2 = 0.971$); a calculated pharmacological half-life for [^{68}Ga]NOTA-RGD of 5.8 min and a calculated elimination rate of 9.1 %ID/h. Urine samples showed steadily accumulating activity levels of [^{68}Ga]NOTA-RGD following a linear incline ($R^2 = 0.967$) peaking at 16 ± 5 %ID/g at 120 min (**Fig. 4b**) with a total urinary recovery reaching 54 ± 4 %ID (N = 3).

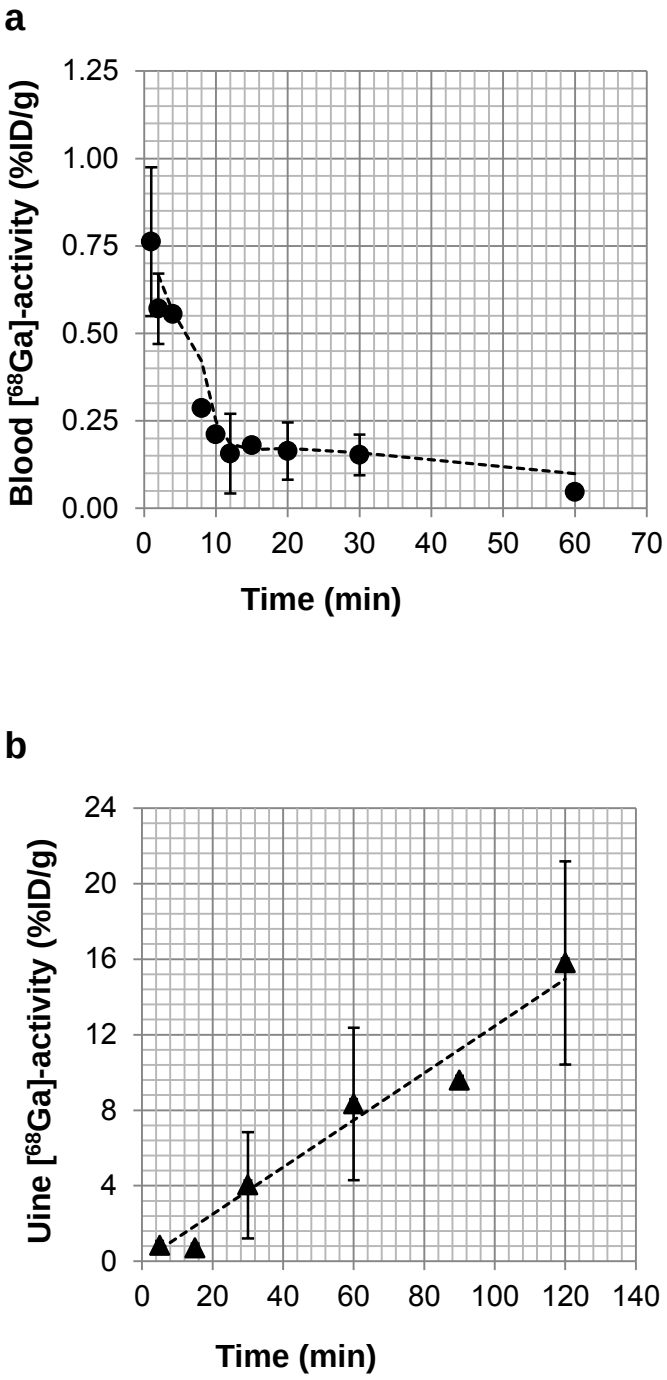

Fig. 4 *Concentration of [^{68}Ga]NOTA-RGD in blood and urine samples from healthy vervet monkeys. Tracer clearance from blood (**a**) assembled as a time-activity curve, follows an exponential decline (R^2 = 0.971) after Savitzky-Golay data smoothing algorithm applied (Origin 8.0 Software). Tracer recovery in urine (**b**) demonstrated a continuous incline (y = 0.125x; R^2 = 0.967). Results are expressed as mean ± SD of three animals and expressed as percentage of the injected [^{68}Ga]-activity per gram (%ID/g). Only at 30, 60 and 90 min more than one sample was taken and hence a standard deviation could be reported.*

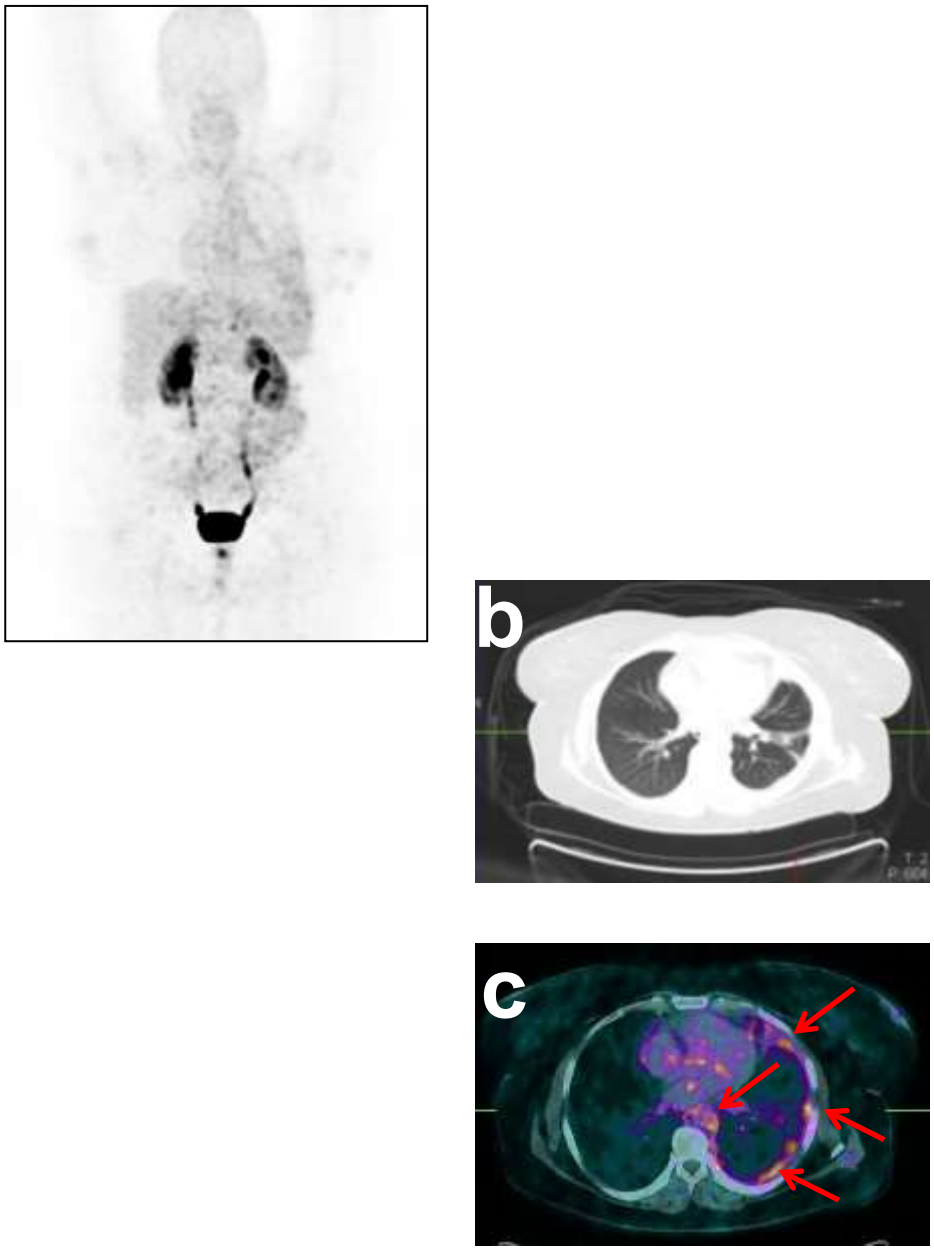

Fig. 5 [^{68}Ga]NOTA-RGD-PET/CT imaging of pulmonary nodular masses of a 51-year-old female with malignant lung pathology. PET (**a**) maximum intensity projection (MIP) showed expected tracer distribution including intense renal excretion at 60 min post injection; the red dotted line indicates position of the axial image slice displayed in (**b**) CT image of lung tissue and (**c**) PET/CT image including [^{68}Ga]NOTA-RGD accumulation in the left lower pleural space showing multiple pulmonary nodules (red arrows) and other organs (heart).

[^{68}Ga]NOTA-RGD Kit Sensitivity towards Detection of SPN in Humans

A full set of quality control measures was performed prior to injection resulting in a pure, sterile and particle-free product solution. Three representative patients are reported to verify the kit performance for future detection of SPN or adjacent lung malignancies. Patients were injected with a 6.5-8.5 mL bolus containing 203.5 -207.2 MBq [^{68}Ga]NOTA-RGD activity (body weight = 50 kg, 90 kg and 100 kg) in saline solution (specific activity = 15.9-16.8 GBq/µmol). A 51-year-old Caucasian female presented with confirmed lung pathology on CT is exemplified for [^{68}Ga]NOTA-RGD-PET/CT (Fig.5). In addition, a 63-year old African male presented with a major lung malignancy consuming the left lung lobe tissue (Suppl. Fig. II a-c) and a 72-year old Caucasian female presented with a confirmed SPN in the right lung lobe (Suppl. Fig I a-c) underwent [^{68}Ga]NOTA-RGD-PET/CT imaging. PET image interpretations showed good overall image quality with notable tracer uptake in heart, liver, spleen, and thyroid, predominant renal excretion ($\%ID_{kidneys\ /\ urinary\ bladder}$ 26 ± 3%, n=3) and some large upper intestinal activity recovery (0.5-3 %ID) (**Fig. 5a** and **Suppl.Fig. Ia, IIa**). The average organ activity concentration (SUV_{mean}) was 1.5 ± 0.2, 1.5 ± 0.2, 1.5± 0.1, 1.9 ± 0.6, 2.1 ± 0.5, 0.4 ± 0.04 and 0.5 ± 0.03 for *arcus aortae*, thyroid, heart, liver, spleen, lung reference tissue and bone marrow (n=3), respectively. All CT image interpretation revealed numerous non-calcified nodular masses in the lower left lung lobe (**Fig. 5b,** and **Suppl. Fig Ib, IIb**) which were congruent with the [^{68}Ga]NOTA-RGD signal in PET (**Fig. 5c** and **Suppl. Fig Ic, IIc**). The peak activity (SUV_{max}) within SPN of the three patients ranged from 2.7 to 4.7 (3.7 ± 0.7, n=11) which allowed for a significant tumor delineation from non-malignant lung tissue (SUV_{max} 0.4 - 0.9, P <0.001).

Discussion

The purpose of this study was to provide nuclear physicians with a kit formulated radiodiagnostic agent that is tested for injection safety, providing information about shelf-life, radiolabeling robustness, stability and purity. In addition, blood and urine pharmacokinetics and biodistribution showed desirable tracer properties in non-human primates, which is still considered a key requirement to administer [^{68}Ga]NOTA-RGD to humans. We have chosen a representative case reporting the uncompromised targeting ability of [^{68}Ga]NOTA-RGD (K60 kits) as a radiodiagnostic agent targeting tumor integrin expression in SPN. Several aspects regarding the current results and the clinical application are discussed as follows: firstly, the main challenge of this study was to evaluate the adaption of an in-house

manufactured NOTA-RGD kit to accommodate ^{68}Ga that was yielded under more acidic conditions from a SnO_2 based [^{68}Ge]/[^{68}Ga]-generator. Secondly, the application of this [^{68}Ga]-labeled RGD conjugate in vervet monkeys has to date not been reported. Lastly, the final product (being complaint with all quality control requirements) was injected into three patients with pulmonary malignancies to allow for PET/CT imaging, thus the kit performance was evaluated based on expected biodistribution and pulmonary lesion detection. As a prerequisite to the herein reported *in vivo* applications we initially studied the kit performance *ex vivo* in an A549-bearing mouse xenograft model to assure the uncompromised targeting abilities of the kit-formulated [^{68}Ga]NOTA-RGD [35]. The animals showed sensitive [^{68}Ga]NOTA-RGD tumor accumulation presenting maximal tumour/muscle and tumor/lung ratios of 6.1 and 5.1 respectively. Recently, adjacent parallel study revealed sensitive targeting behaviour of the kit-labeled [^{68}Ga]NOTA-RGD in case of a 32-year-old male suffering from a chondroblastic osteosarcoma of the skull that was presenting with negative [^{18}F]FDG accumulation [36]. In humans it has already been shown that a tracer such as [^{18}F]FDG PET is superior to RGD for tumor staging, but the relevance stems from the complementary information provided by RGD which justify the need for the availability of angiogenic imaging.

[^{68}Ga]NOTA-RGD Kit Validation

Kit-based radiolabeling techniques are well established procedures for complexation of technetium-99m to radiodiagnostic compounds and recently, generic kit-based techniques have been developed for gallium-68 labeling [37]. We have gained experience with these procedures by establishing a single-vial kit solution for quantitative radiolabeling of ACD-A and PSMA-11 for ^{68}Ga eluted from the same SnO_2 matrix [38-39] as reported herein. Straightforward radiosyntheses are currently available for three [^{18}F]-labeled RGD derivatives [40-42]. From personal experience we know that kit-based radiolabeling protocols are normally not very adaptable to deviations; it has been concluded that the utilization of a different generator type that provides ^{68}Ga from tin-dioxide matrix–bonded [^{68}Ge], is the main reason for the lack of radiolabeling performance. Although gallium-68 is a generator-based radiometal isotope, the isotopes produced by the different generator types available can currently not be handled in the same way, especially when the gallium-68 solution is obtained using different acidic conditions and purification methods [34, 43-45]. In addition, the choice of the ^{68}Ga-chelating agent is of importance as the different chelator molecules incorporate ^{68}Ga with different kinetics, affinities and require different acidities and incubation

temperatures of the reaction mixture [46-48]. To our advantage, RGD has formed part of numerous studies evaluating new generator types, radiolabeling conditions, chelator molecules and bioconjugates. It was plausible to keep NOTA as a chelator; with its three carboxyl and three tertiary amine residues it has been previously demonstrated to robustly complex with soluble gallium-68 [49]. Contrary to DOTA, the NOTA-structure provides better selectivity for gallium-68. The resulting bioconjugate is expected to show superior *in vivo* stability against trans-chelation or blood degradation which would lead to non-specific accumulation of released [^{68}Ga]Ga^{3+}.

The "in-house" NOTA-RGD kit labeling procedure was successfully adapted to ^{68}Ga, which was eluted from a tin dioxide matrix, firstly by fractionated elution - a robust and efficient step to reduce the eluate volume and co-eluted traces of germanium, iron, and zinc [44]. The results from radiolabeling and purification for the [^{68}Ga]NOTA-RGD kit were comparable with the labeling efficiency reported for DOTA-conjugated peptides [33]. The fractionated elution method utilized yielded a very high [^{68}Ga]-activity. However, it has been reported that anionic/cationic exchange cartridge based eluate purifications are more efficient than eluate fractionation [44, 50-53], mainly by reducing co-eluted metal impurities and at the same time it offers an opportunity to eliminate [^{68}Ge] prior to radiolabeling. We have focussed mainly on the concentration effect of the eluate purification method (achieved by a full-scale elution of [^{68}Ga]$GaCl_3$ reduced from 7.5 mL to 0.84 mL) comparable to similar procedures published by *de Blois et al.* [42] which led to higher specific activities of the final product. Using the prescribed anionic-exchange based purification method for the eluate revealed no significant advantage in the %LE (**Tab. 1**). The tendency observed was a slightly higher efficiency in labeling but a significant reduction in the percentage colloid formed (P <0.05). The kit technique allowed the synthesis of [^{68}Ga]NOTA-RGD in a straightforward, one-pot procedure in less than 20 min with a specific activity four times lower compared to the 74 GBq/µmol reported by *Kim et al*. [54] (a three time higher peptide amount was used for a full scale preparation). Using sodium acetate instead of disodium hydrogen phosphate as buffer accomplished [^{68}Ga]NOTA-RGD labeled at room temperatures to yield between 30 and 50% radiolabeled product. However, sufficient labeling efficiencies were achieved at 90 °C (i.e. a 31 to 59% benefit employing heating step; N = 5, P = 0.029). Following radiolabeling a SPE step was required which supported a significant purification of [^{68}Ga]NOTA-RGD from un-chelated ^{68}Ga and [^{68}Ga]-colloids, but also from occult [^{68}Ge] and cationic metal impurities. In addition, SPE eluent solvents such as ethanol or acetonitrile

could be minimized by the choice of an optimal SPE performance which we adapted from a former evaluation [55]. The importance and advantages of this purification step for any potential (pre)clinical application were also emphasized previously [44].

Aside from sterility, consistent appearance, thermodynamic and radiochemical stability, the consideration of the chemical kit stability is a key prerequisite for its successful translation into human application. Normally, larger batches of manufactured kit vials are stored and used on demand, which led us to include the long term stability for NOTA-RGD. The kit integrity was found to be compromised by storage temperatures ($P = 0.008$) of 2-8 °C, thus, at least freezer storage is recommended which ascertains repeatable radiolabeling for approximately two months (**Fig. 2**; $P > 0.05$). This kit approach satisfies the necessity of a standardized pharmaceutical product with controlled quality and wide availability. Implementation to available remote-controlled module based radiosynthesis seems conceivable.

Kit Performance in Non-human Primates and Cancer Patients

Non-human primates are normally employed to translate the use of advanced radiopharmaceuticals to humans. The vervet monkey model as indicated in a recent review [56], is suitable for a spectrum of investigations regarding animal behaviour, metabolism and immunity. With regards to radiolabeled RGD derivatives, very little evidence was found using non-human primates. A SPECT radiotracer [^{99m}Tc]-labeled dimeric RGD was studied in a similar fashion five years ago using non-human primates [57]. Recently, the biodistribution and radiation dosimetry of [^{18}F]RGD-K5 was determined in monkeys and in humans [58]. The whole-body distribution and radiation dosimetry of [^{68}Ga]NOTA-RGD was already clinically assessed in 2012 [54] for its stability, biodistribution and dosimetry. However, to our best knowledge, this study reports the first image-guided biodistribution and pharmacologic investigation of [^{68}Ga]NOTA-RGD using a non-human primate model. This approach will close the crucial gap in the tracer translation to humans and may facilitate better imaging performances. From former experience we know that the monkey model can tolerate the tracer administration and subsequent scanning with no adverse effects [55]. The obtained tracer activity was sufficient for administration of up to 37 MBq/kg in a 7.5 kg monkey to evaluate the *in vivo* biodistribution and to achieve prior information about the *in vivo* tracer stability. The half-life of gallium-68 is relatively short which limits the contamination risk by excretion. In addition, the biodistribution recorded in larger animals

has sufficient resolution on a human PET/CT scanner, similar to paediatric diagnostics. The experimental design allows for sufficient blood and urine collection as opposed to rodent tests, which gives the opportunity to be statistical compliant even though a small number of animals were used. Ethical approval was achieved for 3 animals with a maximum of 3 PET/CT scans per animal. Hence, as much info as possible was derived from the data sets resulting in n=3 for 60 min only. The pharmacokinetic evaluation and the image-guided biodistribution showed rapid blood clearance of the tracer within 60 min post-injection ($P < 0.001$), gradual soft tissue clearance via renal excretion and transient liver uptake. No significant activity was found in potential target organs such as the lungs and the brain. The higher uptake levels in urinary bladder and kidneys dominated the [^{68}Ga]NOTA-RGD biodistribution which is a challenge to detect adjacent tumors in these two areas. This potential limitation often occurs for PET agents; however, there are proven procedures in place to lower the renal radiation level (i.e. voiding the bladder or catheter irrigation) which allows for a less disturbed image interpretation. More than 54% of the injected activity dose was recovered in total urine, 120 min post-injection. Significant increase in urine activity was noted after 15 min ($P < 0.05$). Based on our findings we have reason to believe that uptake, distribution and excretion of NOTA-RGD is very favourable to detect and monitor lung cancer malignancies. It is noted, that the biodistribution showed no significant hepatobiliar excretion and it may therefore be postulated to extend it to the detection of tumors located in the abdomen.

Kit Sensitivity for Detection of SPN in Humans

Advanced lung cancer, including stage III/ IV, that are related to HIV/AIDS are understudied and reported in increasing numbers throughout the African population. A potent imaging agent, which can localize solitary pulmonary lesions and provide specific information towards a potential treatment, is highly desired. We achieved a kit procedure that allows for a cost-efficient and safe radiolabeling of NOTA-RGD as well as subsequent tracer injection into cancer patients. To date, some clinical achievements were accomplished. In 2005, [^{18}F]Galacto-RGD was the first tracer studied in patients with various cancers [59-60]. Over the last decade, RGD became a well studied biomarker of angiogenesis, being clinically evaluated for tumor detection and staging of a broad spectrum of tumors, such as breast cancer, glioblastoma multiforme, non-small renal cell carcinoma, squamous cell carcinoma, melanoma, sarcoma and non-small cell lung cancer [28]. The only reported clinical evidence for [^{68}Ga]NOTA-RGD and [^{68}Ga]NOTA-PRGD2, in particular, is their radiation dosimetry

[54] and recent clinical investigations of [^{68}Ga]NOTA-PRGD2 for prospective imaging of glioma (83% sensitivity, 12 patients) [61] and in patients with lung cancer (selectivity, sensitivity and accuracy >80%) [62]. As [^{68}Ga]NOTA-RGD seems completely unstudied in cancer patients, we have recently reported avid [^{68}Ga]NOTA-RGD uptake in a case of [^{18}F]FDG-PET negative chondroblastic osteosarcoma using this kit radiolabeling procedure [63]. Herein, the NOTA-RGD kit performance was verified for detection of small pulmonary nodules, as presented in a representative patient with confirmed lung pathology based on CT. The unspecific biodistribution of [^{68}Ga]NOTA-RGD did not show any unexpected accumulation and the dominating renal route of tracer excretion 60 min post-injection is in alignment with former reported patient pharmacokinetics of [^{68}Ga]NOTA-PRGD2. However, we report herein lower SUV(mean) values (**Tab. 3**), which seems conclusive, as the pharmacological half-life for NOTA-RGD < NOTA-PRGD2. With regards to sensitive detection of pulmonary abnormalities, the [^{68}Ga]NOTA-RGD kit labeling (specific activity = 8.8-37.9 GBq/µmol) provided similar radiochemical purity in the same incubation time compared to [^{68}Ga]NOTA-PRGD2; the specific activity was well in line with the 9.4-46.3 GBq/µmol reported for [^{68}Ga]NOTA-PRGD2 [64]. PET/CT images (**Fig. 5b, c**) indicated significant delineation of the pulmonary nodules from lung reference tissue (P = 0.006). The SUV values calculated for representative nodules are not significantly lower than those reported for [^{18}F]Galacto-RGD in a study of non-small cell lung cancer (SUV = 0.3-6.8) [9].

Overall, breast cancer seems to be the most studied cancer type with the available RGD radiotracers (50 patients reported 77-100% accuracy) which supports the successful clinical application of RGD in non-invasive imaging. However, lung cancer scenarios are more complex, especially with HIV/AIDS as an underlying disease [65]. Another opportunistic lung disease, tuberculosis, can be the reason for the extraordinary challenge regarding lung cancer as pulmonary lesions caused by tuberculosis might mimic pulmonary cancer [32, 66] in PET.

Limitations

As mentioned earlier, kit-based radiolabeling can be considered a highly successful, but also rigid technique to assure maximum radiolabeling robustness and repeatability. It is of great value for routine (module-based) production. Unfortunately, it will never be a “one-size-fits-all” solution. Radiochemically, the peptide and buffer contents in the kit vial is combined to allow only for a distinct activity concentration to be added and will not tolerate any major

deviations from any set parameter (i.e. change in eluate acidity, incubation duration or temperature) [67]. However, in agreement with our investigation, more generically applicable procedures to label peptides with ^{68}Ga were reported recently [37].

With regards to the avid urinary tracer accumulation, image quality and analysis of tumors in the vicinity of the bladder or kidneys might be compromised. This could lead to impaired visualizing of renal- or prostate cancer. In addition, based on the available clinical results, a lower imaging sensitivity is discussed as a drawback for monomer RGD derivatives as compared to multimer RGD derivatives for localizing tumor metastases [68].

In some circumstances the expression of integrins in normal tissue such as smooth muscle cells or macrophages can be elevated. This might be the reason why there are some reported applications for RGD based radiopharmaceuticals outside the field of oncology; PET/CT imaging using radiolabeled RGD derivatives was employed for studying atherosclerosis [69], rheumatoid arthritis [70] and vascular diseases [71], as angiogenesis is an integral part of repair processes and inflammation and involve neovasculature with activated endothelial cells that highly express integrins. This might be of importance when inconclusive interpretation of oncologic imaging with RGD tracers occurs.

Conclusion

A more flexible radiolabeling procedure using kit-formulated NOTA-RGD that may use ^{68}Ga from different generator types was successfully evaluated. The uncompromised *in vivo* behaviour and efficient targeting of small pulmonary nodules require further clinical investigations. This study may provide an important aspect for the full validation of the clinical relevant [^{68}Ga]NOTA-RGD derivatives to implement guidelines and management of patients with regard to integrin targeted imaging and therapy. Integrin expression comparison with PET/CT or PET/MR may be utilized in the near future.

Acknowledgements

The authors would like to thank the Nuclear Technologies in Medicine and the Biosciences Initiative (NTeMBI), a national technology platform developed and managed by the South African Nuclear Energy Corporation (Necsa) and funded by the Department of Science and Technology. Mrs. B. Mokaleng is thanked for supporting the kit radiolabeling and assistance with the animal experiments. We would further like to thank Mrs. D. van Wyk, Mrs. T.

Pulker and Prof V. Naidoo for their excellent support with the non-human primate study. Prof M. Vorster is thanked for interpretation of the clinical PET/CT images. Mrs V. Satzinger is thanked for providing 3-D-rendered PET/CT images calculated with Siemens in-house software.

Conflicts of Interest

The authors declare no conflict of interest.

References

1. Malvezzi M, Bertuccio P, Levi F et al (2013) European cancer mortality predictions for the year 2013. Annals of oncology : official journal of the European Society for Medical Oncology / ESMO 24:792-800.
2. Parkin DM, Stjernsward J, Muir CS (1984) Estimates of the worldwide frequency of twelve major cancers. Bulletin of the World Health Organization 62:163-182.
3. Ferlay J, Shin HR, Bray F et al (2010) Estimates of worldwide burden of cancer in 2008: GLOBOCAN 2008. International journal of cancer Journal international du cancer 127:2893-2917.
4. Sathekge M, Buscombe JR (2011) Can positron emission tomography work in the African tuberculosis epidemic? Nuclear medicine communications 32:241-244.
5. Pakkala S, Ramalingam SS (2010) Lung cancer in HIV-positive patients. Journal of thoracic oncology : official publication of the International Association for the Study of Lung Cancer 5:1864-1871.
6. Mbulaiteye SM, Parkin DM, Rabkin CS (2003) Epidemiology of AIDS-related malignancies an international perspective. Hematology/oncology clinics of North America 17:673-696, v.
7. Xanthopoulos EP, Corradetti MN, Mitra N et al (2013) Impact of PET staging in limited-stage small-cell lung cancer. Journal of thoracic oncology : official publication of the International Association for the Study of Lung Cancer 8:899-905.
8. Brooks PC, Clark RA, Cheresh DA (1994) Requirement of vascular integrin alpha v beta 3 for angiogenesis. Science 264:569-571.
9. Beer AJ, Lorenzen S, Metz S et al (2008) Comparison of integrin alphaVbeta3 expression and glucose metabolism in primary and metastatic lesions in cancer patients: a PET study using 18F-galacto-RGD and 18F-FDG. Journal of nuclear medicine : official publication, Society of Nuclear Medicine 49:22-29.
10. (2008) The Role of PET/CT in Radiation Treatment Planning for Cancer Patient Treatment. In IAEA Report. International Atomic Energy Agency: Nuclear Medicine Section, p 22.
11. D'Souza SE, Ginsberg MH, Plow EF (1991) Arginyl-glycyl-aspartic acid (RGD): a cell adhesion motif. Trends in biochemical sciences 16:246-250.

12. Conti L, Lanzardo S, Iezzi M et al (2013) Optical imaging detection of microscopic mammary cancer in ErbB-2 transgenic mice through the DA364 probe binding alphav beta3 integrins. Contrast media & molecular imaging 8:350-360.
13. Carman CV (2012) Overview: imaging in the study of integrins. Methods Mol Biol 757:159-189.
14. Cai W, Niu G, Chen X (2008) Imaging of integrins as biomarkers for tumor angiogenesis. Current pharmaceutical design 14:2943-2973.
15. Meyer A, Auernheimer J, Modlinger A, Kessler H (2006) Targeting RGD recognizing integrins: drug development, biomaterial research, tumor imaging and targeting. Current pharmaceutical design 12:2723-2747.
16. Wu Y, Cai W, Chen X (2006) Near-infrared fluorescence imaging of tumor integrin alpha v beta 3 expression with Cy7-labeled RGD multimers. Molecular imaging and biology : MIB : the official publication of the Academy of Molecular Imaging 8:226-236.
17. Mathejczyk JE, Pauli J, Dullin C et al (2011) Spectroscopically well-characterized RGD optical probe as a prerequisite for lifetime-gated tumor imaging. Molecular imaging 10:469-480.
18. Lee J, Lee TS, Ryu J et al (2013) RGD peptide-conjugated multimodal NaGdF4:Yb3+/Er3+ nanophosphors for upconversion luminescence, MR, and PET imaging of tumor angiogenesis. Journal of nuclear medicine : official publication, Society of Nuclear Medicine 54:96-103.
19. Chen X, Sievers E, Hou Y et al (2005) Integrin alpha v beta 3-targeted imaging of lung cancer. Neoplasia 7:271-279.
20. Mondal G, Barui S, Chaudhuri A (2013) The relationship between the cyclic-RGDfK ligand and alphavbeta3 integrin receptor. Biomaterials 34:6249-6260.
21. Haubner R, Wester HJ (2004) Radiolabeled tracers for imaging of tumor angiogenesis and evaluation of anti-angiogenic therapies. Current pharmaceutical design 10:1439-1455.
22. Liu Z, Niu G, Shi J et al (2009) (68)Ga-labeled cyclic RGD dimers with Gly3 and PEG4 linkers: promising agents for tumor integrin alphavbeta3 PET imaging. Eur J Nucl Med Mol Imaging 36:947-957.
23. van Hagen PM, Breeman WA, Bernard HF et al (2000) Evaluation of a radiolabelled cyclic DTPA-RGD analogue for tumour imaging and radionuclide therapy. International journal of cancer Journal international du cancer 90:186-198.
24. Muhlhausen U, Komljenovic D, Bretschi M et al (2011) A novel PET tracer for the imaging of alphavbeta3 and alphavbeta5 integrins in experimental breast cancer bone metastases. Contrast media & molecular imaging 6:413-420.
25. Jeong JM, Hong MK, Chang YS et al (2008) Preparation of a promising angiogenesis PET imaging agent: 68Ga-labeled c(RGDyK)-isothiocyanatobenzyl-1,4,7-triazacyclononane-1,4,7-triacetic acid and feasibility studies in mice. Journal of nuclear medicine : official publication, Society of Nuclear Medicine 49:830-836.
26. Oxboel J, Schjoeth-Eskesen C, El-Ali HH et al (2012) (64)Cu-NODAGA-c(RGDyK) Is a Promising New Angiogenesis PET Tracer: Correlation between Tumor Uptake and Integrin alpha(V)beta(3) Expression in Human Neuroendocrine Tumor Xenografts. International journal of molecular imaging 2012:379807.
27. Notni J, Pohle K, Wester HJ (2013) Be spoilt for choice with radiolabelled RGD peptides: preclinical evaluation of (6)(8)Ga-TRAP(RGD)(3). Nucl Med Biol 40:33-41.
28. Chen H, Niu G, Wu H, Chen X (2016) Clinical Application of Radiolabeled RGD Peptides for PET Imaging of Integrin alphavbeta3. Theranostics 6:78-92.
29. Brechbiel MW (2008) Bifunctional chelates for metal nuclides. The quarterly journal of nuclear medicine and molecular imaging : official publication of the Italian Association of Nuclear Medicine 52:166-173.

30. Jamous M, Haberkorn U, Mier W (2013) Synthesis of peptide radiopharmaceuticals for the therapy and diagnosis of tumor diseases. Molecules 18:3379-3409.
31. Decristoforo C (2012) Gallium-68 -- a new opportunity for PET available from a long shelf-life generator - automation and applications. Current radiopharmaceuticals 5:212-220.
32. Sathekge MM, Maes A, Pottel H et al (2010) Dual time-point FDG PET-CT for differentiating benign from malignant solitary pulmonary nodules in a TB endemic area. South African medical journal = Suid-Afrikaanse tydskrif vir geneeskunde 100:598-601.
33. Rossouw DD, Breeman WA (2012) Scaled-up radiolabelling of DOTATATE with 68Ga eluted from a SnO2-based 68Ge/68Ga generator. Appl Radiat Isot 70:171-175.
34. Breeman WA, de Jong M, de Blois E et al (2005) Radiolabelling DOTA-peptides with 68Ga. Eur J Nucl Med Mol Imaging 32:478-485.
35. Ebenhan T, Schoeman I, Roussow N et al (2014) Qualification of in-house prepared 68Ga-NOTA-RGD kit in mice and monkeys for subsequent molecular imaging of αvβ3 integrin expression in cancer patients. . International Journal of Nuclear Medicine and Molecular Imaging 2014 P23.
36. Orunmuyi A, Modiselle M, Lengana T et al (2016) 68Gallium-Arginine-Glycine-Aspartic Acid and 18F-Fluorodeoxyglucose Positron Emission Tomography/Computed Tomography in Chondroblastic Osteosarcoma of the Skull. Journal of Nucler Medicine and Molecular Imaging [in press].
37. Wangler C, Wangler B, Lehner S et al (2011) A universally applicable 68Ga-labeling technique for proteins. Journal of nuclear medicine : official publication, Society of Nuclear Medicine 52:586-591.
38. Vorster M, Mokaleng B, Sathekge MM, Ebenhan T (2013) A modified technique for efficient radiolabeling of 68Ga-citrate from a SnO2-based 68Ge/68Ga generator for better infection imaging. Hellenic journal of nuclear medicine 16:193-198.
39. Ebenhan T, Vorster M, Marjanovic-Painter B et al (2015) Development of a Single Vial Kit Solution for Radiolabeling of 68Ga-DKFZ-PSMA-11 and Its Performance in Prostate Cancer Patients. Molecules 20:14860-14878.
40. Liu S, Liu H, Jiang H et al (2011) One-step radiosynthesis of (1)(8)F-AlF-NOTA-RGD(2) for tumor angiogenesis PET imaging. Eur J Nucl Med Mol Imaging 38:1732-1741.
41. Liu Z, Li Y, Lozada J et al (2013) Kit-like 18F-labeling of RGD-19F-arytrifluroborate in high yield and at extraordinarily high specific activity with preliminary in vivo tumor imaging. Nucl Med Biol 40:841-849.
42. Wan W, Guo N, Pan D et al (2013) First experience of 18F-alfatide in lung cancer patients using a new lyophilized kit for rapid radiofluorination. Journal of nuclear medicine : official publication, Society of Nuclear Medicine 54:691-698.
43. Fani M, Andre JP, Maecke HR (2008) 68Ga-PET: a powerful generator-based alternative to cyclotron-based PET radiopharmaceuticals. Contrast media & molecular imaging 3:67-77.
44. de Blois E, Sze Chan H, Naidoo C et al (2011) Characteristics of SnO2-based 68Ge/68Ga generator and aspects of radiolabelling DOTA-peptides. Appl Radiat Isot 69:308-315.
45. Chakravarty R, Chakraborty S, Dash A, Pillai MR (2012) Detailed evaluation on the effect of metal ion impurities on complexation of generator eluted (68)Ga with different bifunctional chelators. Nucl Med Biol.
46. Velikyan I (2013) Prospective of (6)(8)Ga-radiopharmaceutical development. Theranostics 4:47-80.
47. Velikyan I (2015) Continued rapid growth in (68) Ga applications: update 2013 to June 2014. Journal of labelled compounds & radiopharmaceuticals 58:99-121.
48. Velikyan I, Maecke H, Langstrom B (2008) Convenient preparation of 68Ga-based PET-radiopharmaceuticals at room temperature. Bioconjugate chemistry 19:569-573.

49. Moore DAF, P.E. ; Welch, M.J. (1990) A novel hexachelating amino-thiol ligand and its complex with gallium(III). Inorganic chemistry 29:4.
50. Zhernosekov KP, Filosofov DV, Baum RP et al (2007) Processing of generator-produced 68Ga for medical application. Journal of nuclear medicine : official publication, Society of Nuclear Medicine 48:1741-1748.
51. Loktionova NS, Belozub AN, Filosofov DV et al (2011) Improved column-based radiochemical processing of the generator produced 68Ga. Appl Radiat Isot 69:942-946.
52. Asti M, De Pietri G, Fraternali A et al (2008) Validation of (68)Ge/(68)Ga generator processing by chemical purification for routine clinical application of (68)Ga-DOTATOC. Nucl Med Biol 35:721-724.
53. Meyer GJ, Macke H, Schuhmacher J et al (2004) 68Ga-labelled DOTA-derivatised peptide ligands. Eur J Nucl Med Mol Imaging 31:1097-1104.
54. Kim JH, Lee JS, Kang KW et al (2012) Whole-body distribution and radiation dosimetry of (68)Ga-NOTA-RGD, a positron emission tomography agent for angiogenesis imaging. Cancer biotherapy & radiopharmaceuticals 27:65-71.
55. Ebenhan T, Govender T, Kruger G et al (2012) Synthesis of 68Ga-NOTA-UBI30-41 and in vivo biodistribution in vervet monkeys towards potential PET/CT imaging of infection. Journal of nuclear medicine : official publication, Society of Nuclear Medicine 53:1520.
56. Jasinska AJ, Schmitt CA, Service SK et al (2013) Systems biology of the vervet monkey. ILAR journal / National Research Council, Institute of Laboratory Animal Resources 54:122-143.
57. Jia B, Liu Z, Zhu Z et al (2011) Blood clearance kinetics, biodistribution, and radiation dosimetry of a kit-formulated integrin alphavbeta3-selective radiotracer 99mTc-3PRGD 2 in non-human primates. Molecular imaging and biology : MIB : the official publication of the Academy of Molecular Imaging 13:730-736.
58. Doss M, Kolb HC, Zhang JJ et al (2012) Biodistribution and radiation dosimetry of the integrin marker 18F-RGD-K5 determined from whole-body PET/CT in monkeys and humans. Journal of nuclear medicine : official publication, Society of Nuclear Medicine 53:787-795.
59. Beer AJ, Haubner R, Goebel M et al (2005) Biodistribution and pharmacokinetics of the alphavbeta3-selective tracer 18F-galacto-RGD in cancer patients. Journal of nuclear medicine : official publication, Society of Nuclear Medicine 46:1333-1341.
60. Haubner R, Weber WA, Beer AJ et al (2005) Noninvasive visualization of the activated alphavbeta3 integrin in cancer patients by positron emission tomography and [18F]Galacto-RGD. PLoS medicine 2:e70.
61. Li D, Zhao X, Zhang L et al (2014) (68)Ga-PRGD2 PET/CT in the evaluation of Glioma: a prospective study. Molecular pharmaceutics 11:3923-3929.
62. Zheng K, Liang N, Zhang J et al (2015) 68Ga-NOTA-PRGD2 PET/CT for Integrin Imaging in Patients with Lung Cancer. Journal of nuclear medicine : official publication, Society of Nuclear Medicine 56:1823-1827.
63. Orunmuyi A, Modiselle M, Lengana T et al (2016) 68Gallium-Arginine-Glycine-Aspartic Acid and 18F-Fluorodeoxyglucose Positron Emission Tomography/Computed Tomography in Chondroblastic Osteosarcoma of the Skull. Journal of Nucler Medicine and Molecular Imaging [in press].
64. Lang L, Li W, Guo N et al (2011) Comparison study of [18F]FAl-NOTA-PRGD2, [18F]FPPRGD2, and [68Ga]Ga-NOTA-PRGD2 for PET imaging of U87MG tumors in mice. Bioconjugate chemistry 22:2415-2422.
65. Sathekge M, Maes A, Al-Nahhas A et al (2009) What impact can fluorine-18 fluorodeoxyglucose PET/computed tomography have on HIV/AIDS and tuberculosis pandemic? Nuclear medicine communications 30:255-257.

66. Sathekge M, Maes A, Kgomo M et al (2011) Use of 18F-FDG PET to predict response to first-line tuberculostatics in HIV-associated tuberculosis. Journal of nuclear medicine : official publication, Society of Nuclear Medicine 52:880-885.
67. Mukherjee A, Pandey U, Chakravarty R et al (2014) Development of single vial kits for preparation of (68)Ga-labelled peptides for PET imaging of neuroendocrine tumours. Molecular imaging and biology : MIB : the official publication of the Academy of Molecular Imaging 16:550-557.
68. Dijkgraaf I, Yim CB, Franssen GM et al (2011) PET imaging of alphavbeta(3) integrin expression in tumours with (6)(8)Ga-labelled mono-, di- and tetrameric RGD peptides. Eur J Nucl Med Mol Imaging 38:128-137.
69. Beer AJ, Pelisek J, Heider P et al (2014) PET/CT imaging of integrin alphavbeta3 expression in human carotid atherosclerosis. JACC Cardiovascular imaging 7:178-187.
70. Zhu Z, Yin Y, Zheng K et al (2014) Evaluation of synovial angiogenesis in patients with rheumatoid arthritis using (6)(8)Ga-PRGD2 PET/CT: a prospective proof-of-concept cohort study. Annals of the rheumatic diseases 73:1269-1272.
71. Choi H, Phi JH, Paeng JC et al (2013) Imaging of integrin alpha(V)beta(3) expression using (68)Ga-RGD positron emission tomography in pediatric cerebral infarct. Molecular imaging 12:213-217.

Supplementary Information

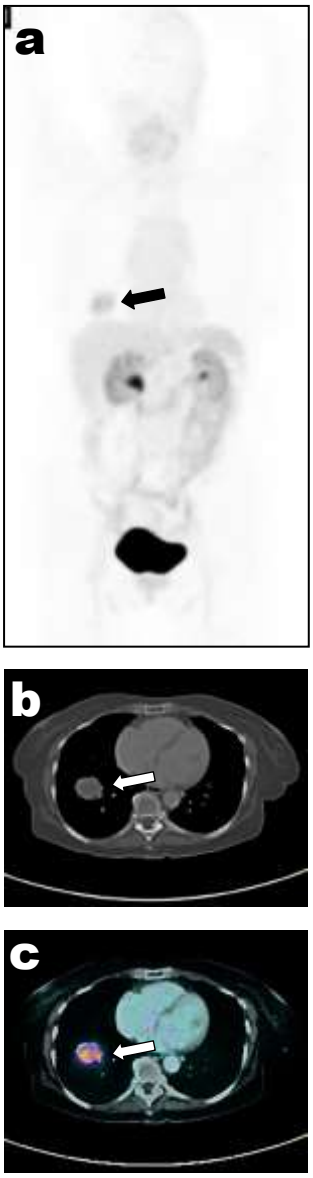

Supplement Fig. I [^{68}Ga]NOTA-RGD-PET/CT imaging of confirmed lung pathology in a 74-year-old female. PET (**a**) maximum intensity projection (MIP) image showed expected tracer distribution including high amounts of activity represented in the bladder at 60 min post injection of 207.2 MBq tracer; (**b**) the axial image slice displayed in the CT image shows the lower right lung lobe area where the tissue abnormality was detected (**c**) the axial PET/CT image showed intense [^{68}Ga]NOTA-RGD uptake co-localizing in the solitary pulmonary nodule (see arrows).

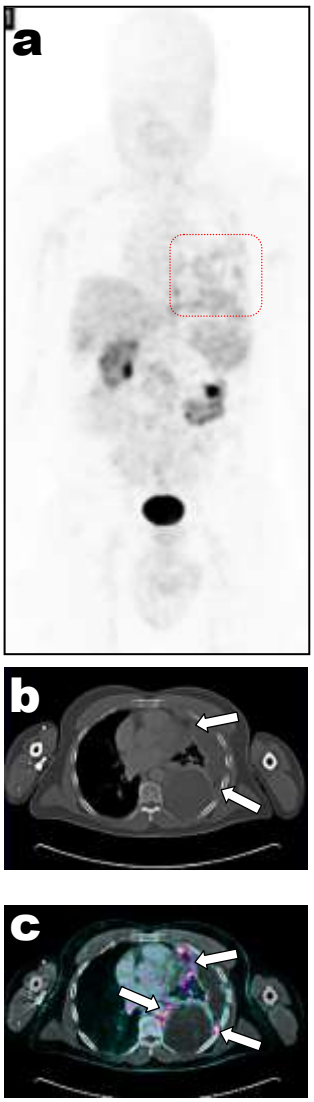

Supplement Fig. II [^{68}Ga]NOTA-RGD-PET/CT imaging of confirmed lung pathology in a 63-year-old male patient. PET (**a**) maximum intensity projection (MIP) image showed expected tracer distribution including intense activity in the bladder at 60 min post injection of 205.4 MBq tracer; the activity surrounded by the red-dotted square represents a massive lung abnormality consuming the left lung lobe adjacent to the heart muscle (**b**) the axial CT image of lung tissue showing abnormal lung tissue localized throughout the dorsal and lateral left lobe (**c**) PET/CT image showed intense nodular [^{68}Ga]NOTA-RGD uptake in the solitary pulmonary nodule (see arrows) in the circumvent of the tumor, in particular.

Gallium-68 Radiolabeling of NOTA-NCS-RGD Kits

We kindly received radiodiagnostic agent kit vials formulated for subsequent ^{68}Ga complexation, developed by Seoul National University, containing 10 nmol NOTA-NCS-RGD in a disodium hydrogen phosphate buffer that showed promising targeting performance to human integrin *in vitro* and to ischemic- and SNU-C4 tumor bearing mice *in vivo* [1]. Despite our best efforts, we did not manage to yield a pure enough [^{68}Ga]-product for our envisaged applications.

Based on HPLC and ITLC analysis the NOTA-NCS-RGD kits from Seoul National University showed 15-65 % labeling efficiencies (N =11). During the purification procedure a complete adsorption of the activity to the dedicated cartridge unit matrix (SPE Alumina N, Waters, Eschborn, Germany) occurred. The HPLC analysis showed multiple radioactive peaks aside from activity that was congruent with the UV signal for NOTA-NCS-RGD. An overall high colloid forming tendency was observed, amounting to 37 ± 13% using ITLC. The alteration of the labeling parameters ([^{68}Ga]-eluate purification, additional buffering solution, molarity or volume of [^{68}Ga]-solution, pH and the incubation duration or temperature) did not positively affect the radiolabeling yield or enabled any purification.

Supplementary Reference

1. Jeong JM, Hong MK, Chang YS et al (2008) Preparation of a promising angiogenesis PET imaging agent: 68Ga-labeled c(RGDyK)-isothiocyanatobenzyl-1,4,7-triazacyclononane-1,4,7-triacetic acid and feasibility studies in mice. Journal of nuclear medicine : official publication, Society of Nuclear Medicine 49:830-836.